Vol. 610: 15–31, 2019
https://doi.org/10.3354/meps12857

MARINE ECOLOGY PROGRESS SERIES
Mar Ecol Prog Ser

Published February 1

Coastal waters freshening and extreme seasonality affect organic matter sources, quality, and transfers in a High Arctic fjord (Young Sound, Greenland)

Guillaume Bridier[1,*], Tarik Meziane[2], Jacques Grall[1,3], Laurent Chauvaud[1], Mikael Kristian Sejr[4,5], Sylvain Menneteau[1,2], Frédéric Olivier[2,6]

[1]Laboratoire des Sciences de l'Environnement Marin (LEMAR) UMR 6539 UBO/CNRS/IRD/Ifremer, rue Dumont D'Urville, 29280 Plouzané, France
[2]Biologie des Organismes et Ecosystèmes Aquatiques (BOREA) UMR 7208 MNHN/CNRS/IRD/SU/UCN/UA, 61 Rue Buffon CP53, 75005 Paris, France
[3]Observatoire Marin, UMS 3113, Institut Universitaire Européen de la Mer, rue Dumont D'Urville, 29280 Plouzané, France
[4]Arctic Research Centre, Aarhus University, Ny Munkegade bldg. 1540, 8000 Aarhus C, Denmark
[5]Department of BioScience, Aarhus University, Vejlsøvej 25, 8600 Silkeborg, Denmark
[6]Station Marine de Concarneau, Muséum National d'Histoire Naturelle, Place de la Croix, 29900 Concarneau, France

ABSTRACT: Arctic benthic ecosystems are expected to experience strong modifications in the dynamics of primary producers and/or benthic–pelagic coupling under climate change. However, lack of knowledge about the influence of physical constraints (e.g. ice-melting associated gradients) on organic matter sources, quality, and transfers in systems such as fjords can impede predictions of the evolution of benthic–pelagic coupling in response to global warming. Here, sources and quality of particulate organic matter (POM) and sedimentary organic matter (SOM) were characterized along an inner–outer gradient in a High Artic fjord (Young Sound, NE Greenland) exposed to extreme seasonal and physical constraints (ice-melting associated gradients). The influence of the seasonal variability of food sources on 2 dominant filter-feeding bivalves (*Astarte moerchi* and *Mya truncata*) was also investigated. Results revealed the critical impact of long sea ice/snow cover conditions prevailing in Young Sound corresponding to a period of extremely poor and degraded POM and SOM. Freshwater inputs had a very local impact during summer, with relatively more degraded POM at the surface compared to bottom waters that were less nutritionally depleted but more heterogeneous among the sampled stations. Terrestrial inputs contributed to the SOM composition but showed a large variability along the fjord. Finally, diet analyses underlined the contrasted nutritional conditions, showing much higher lipid reserves in *A. moerchi* than in *M. truncata* during winter. Under a scenario with increased freshwater input, such results suggest a decline in organic matter quality and production in Young Sound, with subsequent impacts on benthic food webs.

KEY WORDS: Arctic ecosystems · Benthic–pelagic coupling · Organic matter · Climate change · Fatty acids · Stable isotopes · Young Sound

1. INTRODUCTION

The Arctic has been subjected to atmospheric warming in recent decades at a rate that exceeds the global average by a factor of 2–3 (AMAP 2017). This warming has induced major modifications in the Arctic marine environment, e.g. a decrease in sea-ice cover (extent and thickness) and an increase in freshwater discharge (AMAP 2017, Kwok & Rothrock 2009, McPhee et al. 2009, Ohashi et al.

---

*Corresponding author: guillaume.bridier@live.ie

2016). The Greenland Ice Sheet annual net loss is currently estimated at 186 gigatonnes (Gt) yr^{-1}, which is double the melting rate observed for 1983–2003 (Bamber et al. 2012, Kjeldsen et al. 2015). Such changes are expected to impact marine systems through shifts in the spatial distribution of species (Falk-Petersen et al. 2007) and altered food web dynamics via modified quantity, quality, and seasonal timing of primary productivity (Iken et al. 2010, Leu et al. 2011, Ardyna et al. 2014, Arrigo & van Dijken 2015). Moreover, changes in the phenology of primary producers may create mismatches between peak algal blooms and faunal reproductive phases, with major effects on benthic–pelagic coupling (Søreide et al. 2010, Moran et al. 2012).

Several authors have modeled the evolution of food webs and marine wildlife within a changing Arctic (e.g. Wassmann 2011, Kędra et al. 2015). However, recent studies indicate a regionally variable Arctic ecosystem response to global warming depending on specific habitat characteristics (e.g. water depth, exposure to terrestrial runoff; Carmack et al. 2015, De Cesare et al. 2017, Gaillard et al. 2017). For instance, although the generally accepted paradigm states an increase in primary production in the Arctic Ocean, the opposite trend could occur in coastal areas (which represent 35% of the world's coastline) such as fjord systems, due to the increase in freshwater inputs and subsequent turbidity (Carmack et al. 2015, Middelbo et al. 2018). Terrestrial runoff from melting snow and ice increases water column turbidity and diminishes light availability, in turn decreasing primary productivity (Murray et al. 2015, Arimitsu et al. 2016). Freshwater inputs also reduce primary productivity in some fjords due to increased stratification, causing nutrient depletion in surface waters (Piquet et al. 2014, Meire et al. 2016, Middelbo et al. 2018). On the other hand, freshwater inputs from glacier melting may provide labile organic carbon, which may be a source of bioavailable carbon in low-productivity ecosystems (Lawson et al. 2014). The impact of increased freshwater loads on the quality of organic matter and transfers in Arctic fjords remains poorly understood.

We conducted a sampling program during August 2016 and May 2017 in a High Arctic fjord (Young Sound, NE Greenland) to study how seasonal and physical constraints drive the sources and qualitatively change the organic matter available for dominant benthic primary consumers: the abundant filter-feeding bivalves *Astarte moerchi* and *Mya truncata* (Sejr et al. 2000, Born et al. 2003). Potential bivalve food sources and body tissues were analyzed for fatty acid (FA) and stable isotope (SI) composition. FA analysis can be used to trace the origin of organic matter within an environment, since primary producers often show contrasting FA profiles according to their taxonomic group (e.g. diatoms, dinoflagellates, macroalgae; Meziane & Tsuchiya 2000, Dalsgaard et al. 2003, Kelly & Scheibling 2012). Moreover, biosynthesis of specific FAs, such as polyunsaturated FAs (PUFAs), is usually limited in marine bivalves. This enables the use of FA trophic markers to study diet (Kelly & Scheibling 2012, Thyrring et al. 2017). SI analysis may also help to characterize the trophic diet of organisms (Fry 2006, Gaillard et al. 2017) and to investigate environmental processes occurring within an ecosystem, such as inputs of terrestrial carbon (Calleja et al. 2017), organic matter degradation (McTigue et al. 2015), or the dynamics of blooms (Tamelander et al. 2009).

The main goals of this study were to (1) understand how seasonal and physical constraints in Young Sound may influence the sources and quality of particulate organic matter (POM) and sedimentary organic matter (SOM), (2) assess the seasonal patterns (ice/snow cover in May vs. open sea in August) of organic matter transfers within this fjord, and (3) investigate the response of 2 dominating bivalve species (*A. moerchi* and *M. truncata*) to such seasonality in food availability.

2. MATERIALS AND METHODS

2.1. Study site and sampling

The study was conducted in Young Sound (74° N, 20° W, Fig. 1), a High Arctic Greenland fjord characterized by a long sea-ice duration of 9–10 mo (Glud et al. 2007). The fjord is approximately 90 km long and 2–7 km wide. The maximum depth is 330 m, but exchange with coastal waters is limited by a shallow sill with a depth of 45 m at the mouth of the fjord (Bendtsen et al. 2007). During land-glacier and snow melting, the surface waters become more turbid and brackish due to freshwater inputs, especially in the inner part of the fjord (Ribeiro et al. 2017). Generally, such freshwater inputs generate a bilayer estuarine water circulation with low-salinity surface flows from the inner to the outer fjord and inflows occurring close to the seabed (Bendtsen et al. 2014). Young Sound has the typical surface cur-

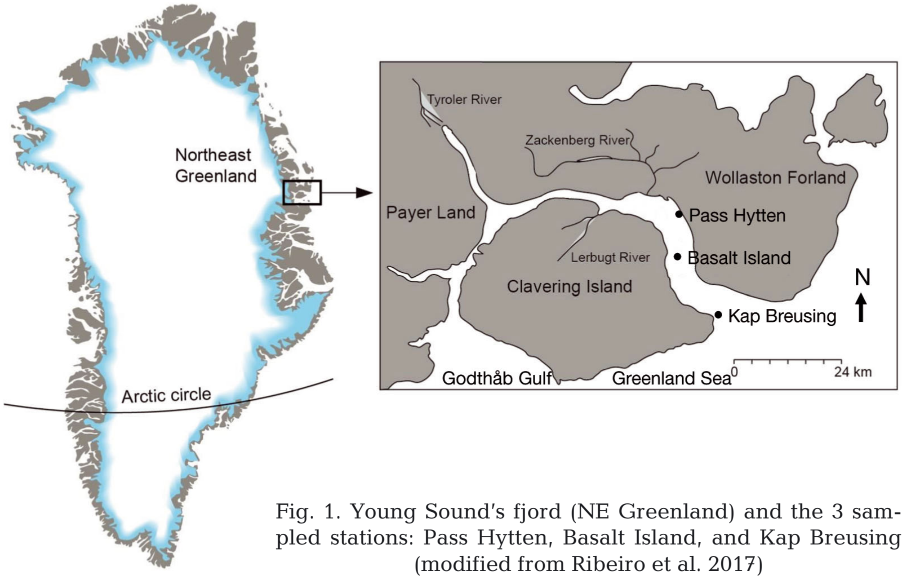

Fig. 1. Young Sound's fjord (NE Greenland) and the 3 sampled stations: Pass Hytten, Basalt Island, and Kap Breusing (modified from Ribeiro et al. 2017)

rent circulation in fjords affected by the Coriolis effect, with the southern part (Clavering Island side) more exposed to freshwater outflow than the northern part (Wolloston Forland side; Bendtsen et al. 2007).

Sampling was conducted in August 2016 (open water, early productive period; De Cesare et al. 2017) and May 2017 (ice cover, expected 'unproductive' period). We sampled 3 stations in 2016 (Fig. 1), i.e. Pass Hytten (depth = 18 m, 74.41° N, 20.33° W), Basalt Island (depth = 21.5 m, 74.33° N, 20.36° W), and Kap Breusing (depth = 20 m, 74.21° N, 20.11° W), but only Pass Hytten and Basalt Island during 2017 for logistical reasons. At each station, 10 l of seawater was collected at 2 depths corresponding to the surface (s-POM, 1 m below the surface) or bottom (b-POM, 1 m above the seabed), using two 5 l Niskin bottles sample^{-1}. In parallel, SOM samples were collected at the sediment surface (~625 cm^2) by SCUBA divers using a 450 ml syringe. Also, several individuals of *Astarte moerchi* and *Mya truncata* were harvested either by SCUBA diving or using a triangular biological dredge (KC Denmark) during both seasons. In addition, 3 macroalgae species (*Desmarestia aculeata*, *Fucus* sp., and *Saccharina latissima*) were harvested during summer in order to assess their potential contribution to the bivalves' diet. Statistical analyses were performed on our own results as well as some raw data previously published in De Cesare (2016) and De Cesare et al. (2017) relating summer samples of *A. moerchi* (SI signatures and FA profiles) and macroalgae (SI signatures).

2.2. Analyses of samples

2.2.1. Preliminary treatments

POM samples were obtained by filtering collected water on precombusted GF/F Whatman® microfiber filters (diameter: 47 mm; pore size: 0.7 µm) until clogging when possible (mean filtered volume: 7.9 ± 1.9 l, range: 4–8 l). Because syringe-collected samples were comprised of a mixture of SOM, inorganic particles, and seawater, we let the samples settle for 1 h prior to filtering the supernatants until clogging on GF/F filters (mean volume: 0.260 ± 0.100 ml, range: 100–450 ml) in order to remove most inorganic sedimentary particles. In the field, all samples were directly frozen at −80°C and transferred to the lab for further analyses. Once in the lab, all samples (i.e. POM and SOM filters as well as digestive glands and muscles) were freeze-dried at −50°C for at least 5 h (30 h for animal tissues) and directly weighed. The POM and SOM filters were cut in 2 parts to perform both FA and SI analyses on the same sample. Each half-filter was weighed and the quantity of organic matter for the FA and SI analysis was calculated by:

$$M(X) = \frac{W_{\text{Half filter}}}{W_{\text{Whole filter}}} \times (W_{\text{Whole filter}} - W_{\text{Precombusted filter}}) \quad (1)$$

where $M(X)$ is the mass (mg) of POM or SOM used for the FA or SI analysis and W is the dried weight of the half, whole, or precombusted filters.

2.2.2. FA analysis

The method used for the FA extraction largely follows the Bligh & Dyer (1959) method as adjusted in Meziane & Tsuchiya (2002). To quantify the FA concentrations, a known volume of a commercial standard (23:0, concentration of 5 mg ml^{-1}) was introduced in each sample. Half-filters for POM and SOM analyses were diluted in a distilled water–chloroform–methanol solution (1:1:2, v:v:v) and sonicated for 20 min for the FA extraction. The samples were then completed by a distilled water–chloroform solution (1:1, v:v) and centrifuged (1409 × g, 5 min). Lipid phases were transferred to separate tubes, completed by a distilled water–chloroform solution (1:1, v:v), and sonicated again for 20 min to maximize the extraction. Then, samples were evaporated under a dinitrogen (N_2) flux, diluted a second time in a mixture of methanol and sodium hydroxide (2:1, v:v; [NaOH] = 2 mol l^{-1}), and heated at 90°C for 90 min for FA saponification. Finally, FAs were converted into FA methyl esters (FAMEs) after incubation for 10 min at 90°C in a methanolic boron trifluoride solution (BF_3–CH_3OH 14%, 1 ml). At the end of the reaction, the chloroform phase containing FAs was retrieved and stored at −20°C.

The FAs were quantified by gas chromatography (Varian CP-3800 equipped with a Supelco® Omegawax® Capillary GC 320 column [length: 30 m; inside diameter: 0.32 mm; film thickness: 0.25 µm], He as carrier gas). FA peaks were identified by comparing with those from an analytical standard (Supelco® 37 Component FAME Mix) and confirmed by mass spectrometry (Varian 220-MS coupled to a Varian 450-GC, He as carrier gas). FA nomenclature is defined as X:YωZ, where X is the number of carbon atoms, Y is the number of double bonds, and Z is the position of the last double bond from the methyl group. The 23:0 standard allowed converting each FAME area into a concentration using (Schomburg 1987):

$$C_{\text{FA}} = \left(\frac{A_{\text{FA}}}{A_{\text{C23}}} \times \frac{C_{23}}{M_f}\right) \quad (2)$$

where C_{FA} is the FA concentration (µg g^{-1}), A_{FA} is the FA peak area, A_{C23} is the 23:0 peak area, C_{23} is the 23:0 quantity (µg) added to each sample, and M_f is the mass of matter deposited on the analyzed half-filter.

The analytical precision for the samples was generally less than 5% for the total amounts and major components of FA (T. Meziane pers. obs.). Table 1 lists all the FAs used as organic matter tracers in this study and their related biomarker information.

2.2.3. SI analysis

SI analysis was performed on the second half of each POM and SOM filter and on *A. moerchi* and *M. truncata* tissues. Half-filters were fumigated for at least 4 h with 35% HCl to remove inorganic carbon (Lorrain et al. 2003). The surface layer, including filtered POM (or SOM), was scraped and 10–30 mg of material was placed in tin capsules. Due to the small amounts of inorganic carbon in digestive glands and muscles, no acidification was performed with these tissues (Jacob et al. 2005, Søreide et al. 2006). The animal tissues were ground and approximately 1 mg was placed in a single tin capsule for each sample. Macroalgae were ground and separated into 2 subsamples (De Cesare et al. 2017): one subsample was acidified (1 M HCl) to remove inorganic carbon and placed in silver capsules for $\delta^{13}C$ analysis, while the second subsample was directly placed in tin capsules (without prior acidification) for $\delta^{15}N$ analysis.

All samples were analyzed at the University of California Davis Stable Isotope Facility (Department of Plant Sciences, UC Davis) by continuous flow isotope ratio mass spectrometry. The equipment consisted of an elemental analyzer (PDZ Europa ANCA-GSL, Sercon; and Elementar Vario EL Cube elemental analyzer, Elementar Analysensysteme; for animal tissue and filter analysis, respectively) interfaced to an isotope ratio mass spectrometer (PDZ Europa 20-20, Sercon). Several replicates of laboratory standards, compositionally similar to analyzed samples and calibrated against NIST Standard Reference

Table 1. Fatty acids (FAs) used in this study as markers to describe the origin and quality of organic matter. SFA: saturated FAs; PUFA: polyunsaturated FAs; EFA: essential FAs

Fatty acids (FAs)	Descriptor of	References
Organic matter origin		
16:1ω7, 16:4ω1, 20:5ω3	Diatoms	Reuss & Poulsen (2002), Dalsgaard et al. (2003), Kelly & Scheibling (2012)
18:4ω3, 22:6ω3	Dinoflagellates	Napolitano et al. (1997), Kelly & Scheibling (2012)
18:2ω6, 18:3ω3, 18:4ω3, 20:5ω3	Macroalgae (Phaeophyceae)	Kelly & Scheibling (2012), De Cesare et al. (2017), Gaillard et al. (2017)
Organic matter quality		
Dominance of SFA (e.g. 14:0, 16:0, 18:0)	Degraded organic matter	Rhead et al. (1971), Connelly et al. (2015), Connelly et al. (2016)
Dominance of PUFA and EFA (here, sum of 20:4ω6, 20:5ω3, and 22:6ω3)	Labile and nutritionally rich organic matter	Soudant et al. (1996), Parrish et al. (2005), Parrish (2009)

Materials (IAEA-600, USGS-40, USGS-41, USGS-42, USGS-43, USGS-61, USGS-64, and USGS-65), were inserted between some of the filter and animal samples to correct deviations occurring during the analysis. The standard deviation of the stable isotope measurements was estimated as ±0.2‰ for $\delta^{13}C$ and ±0.3‰ for $\delta^{15}N$ (UC Davis Stable Isotope facility pers. com.). Carbon and nitrogen isotopic ratios were expressed in per mille (‰) and calculated from international standards (Vienna Pee Dee Belemnite and air, respectively) by:

$$\delta X = \left[\left(\frac{R_{\text{sample}}}{R_{\text{standard}}}\right) - 1\right] \times 1000 \tag{3}$$

where δX is $\delta^{13}C$ or $\delta^{15}N$, and R is the corresponding $^{13}C/^{12}C$ or $^{15}N/^{14}N$ ratio (Peterson & Fry 1987).

2.3. Data analyses

Since pelagic and benthic components usually show different organic matter sources and qualities (e.g. Magen et al. 2010, Kuliński et al. 2014), we chose to separate the SOM and POM samples for statistical analyses. Because our design was not balanced between the 2 seasons (2 stations sampled in winter vs. 3 in summer), we used 2-way permutational multivariate analysis of variance (PERMANOVA) for each season to study the effects of depth (surface or bottom waters) and station factors on the FA profiles of POM. Since PERMANOVAs are not affected by small differences in dispersion, especially with a balanced design, the permutational analysis of multivariate dispersions (PERMDISP) test was performed to ensure that data dispersion, possibly highly heterogeneous, would not disturb the interpretation of our analysis (Anderson et al. 2008, Anderson & Walsh 2013).

Seasonal differences in FA concentrations were tested by 1-way ANOVA, whereas depth and station effects were tested by 2-way ANOVA for each season. FA concentrations were log-transformed prior each analysis to validate normality and homoscedasticity assumptions. When significant effects were detected, pairwise Tukey tests were used to determine if the differences were observed among all groups. Similar analyses were performed on carbon and nitrogen isotopic ratios, with either two 2-way ANOVAs (depth and stations as factors) or one 1-way ANOVA (season as factor), as well as with pairwise tests if needed.

Regarding FA data in animal tissues, homoscedasticity and normality were rarely observed between the 2 factors (e.g. digestive glands from May vs. muscles from August). As data transformation is not recommended for percentage values not derived from count data (as percentage of lipids), we thus performed a 1-way PERMANOVA to test each factor separately (e.g. season was tested for each tissue from a single species). Data from the SI analysis on animal tissue were treated similarly with 1-way ANOVAs. All statistical analyses were performed using R software (R Core Team 2017).

3. RESULTS

3.1. FA profiles from POM and SOM samples

3.1.1. POM

A total of 65 FAs were identified in POM and SOM samples (44 FAs in August and 47 in May). Only FA percentages higher than 0.2% in at least one sample are shown in Table 2. Strong seasonal differences were observed in the FA profiles of the POM samples. For example, apart from s-POM from Basalt Island, the total percentage of PUFAs was between 9.7 and 22.1% in August and was always less than 1.5% in May. Concomitantly, the sum of saturated FAs (ΣSFA) shows opposite seasonal variations, with higher values in May (range: 82.5–93.1%) compared to August (range: 49.5–69.3%).

In August, the FA profiles of the POM samples differed significantly depending on site and depth ($p < 0.01$) and without any interaction between these factors (Table 3). The depth variations in the POM FA profiles were not similar between stations. In fact, the FA profiles of s-POM and b-POM samples from Pass Hytten were rather similar (similarity = 73.1%), but those from Basalt Island differed more with depth (e.g. 18:1ω9 = 1.9 and 6.2% for s-POM and b-POM, respectively; Table 2). In samples from Kap Breusing, the FA profiles strongly differed between surface and bottom waters (similarity = 64.2%) with 20:5ω3 percentages higher in b-POM than in s-POM (9 vs. 2.7%, respectively; Table 2). Considering spatial variability, FA profiles related to the s-POM from Basalt Island in August (Table 2) revealed much more degraded organic matter compared to those from other stations, with a higher sum of SFAs (84.4%), a lower sum of PUFAs (3.1%), and a much lower FA concentration (2.6 mg g^{-1}) than in Pass Hytten and Kap Breusing (8.0 and 9.4 mg g^{-1}, respectively; pairwise test: $p < 0.001$). In contrast, the b-POM samples were rather similar between Basalt Island and Pass Hytten, while those from Kap

Table 2. Fatty acid (FA) composition of particulate organic matter (POM) and sedimentary organic matter (SOM) from summer (August) and winter (May) seasons. s-POM: surface POM; b-POM: bottom POM; SFA: saturated FA; MUFA: monounsaturated FA; PUFA: polyunsaturated FA; BrFA: branched FA; EFA: essential FA; nd: not detected; tr: trace (FA percentage <0.2%). Standard deviations are represented within brackets. FAs with percent-ages lower than 0.2% in all samples are not included in this table

FA	August							May				
	Pass Hytten		Basalt Island		Kap Breusing		SOM	Pass Hytten		Basalt Island		SOM
	s-POM n = 5	b-POM n = 5	s-POM n = 5	b-POM n = 4	s-POM n = 5	b-POM n = 4	n = 10	s-POM n = 4	b-POM n = 4	s-POM n = 5	b-POM n = 5	n = 9
12:0	nd	nd	nd	nd	nd	nd	nd	1.6 (0.7)	3.7 (1.3)	6.6 (4.8)	2.4 (0.6)	1.6 (1.1)
13:0	nd	nd	nd	nd	nd	nd	nd	tr	0.3 (0.2)	tr	tr	0.3 (0.1)
14:0	17.8 (6.2)	7.1 (1.6)	19.9 (7)	8.5 (1.6)	12.9 (3.6)	8.4 (0.8)	9.7 (3.7)	7.5 (0.3)	7.4 (0.9)	13.2 (2.7)	9 (1)	6.3 (1.7)
15:0	1.3 (0.3)	1.8 (0.3)	1.5 (0.3)	2.1 (0.5)	1.3 (0.3)	1.3 (0.2)	1 (0.3)	2.7 (0.3)	2.3 (0.4)	2.5 (0.4)	2.8 (0.5)	1.7 (0.3)
16:0	35.3 (9.8)	32.9 (4.9)	45.1 (8.7)	36 (7.9)	31.5 (3.3)	27.1 (4.8)	34.2 (6.4)	43 (0.8)	41.1 (1.7)	38.6 (5.3)	39.5 (6.3)	46 (3)
17:0	0.8 (0.2)	1.1 (0.2)	1.1 (0.5)	1.5 (0.6)	0.8 (0.2)	0.8 (0.2)	0.6 (0.6)	1.6 (0.1)	1.3 (0.1)	1.3 (0.2)	1.6 (0.3)	1.3 (0.2)
18:0	7.5 (2.8)	20.1 (4.2)	13.5 (4.8)	17.6 (3.4)	8.7 (1.3)	9.8 (2)	9 (7.7)	31.8 (3)	30.5 (6.4)	21.6 (3.7)	22.5 (3.4)	30.5 (4.2)
19:0	0.5 (0.2)	0.3 (0.2)	0.7 (0.2)	0.9 (0.5)	0.5 (0.1)	0.3 (0.2)	0.5 (0.5)	nd	nd	tr	nd	nd
20:0	0.3 (0.1)	0.9 (0.1)	0.5 (0.4)	0.8 (0.2)	0.5 (0.2)	0.5 (0.1)	0.4 (0.4)	1.6 (0.0)	1.3 (0.1)	1.1 (0.2)	1.2 (0.1)	1.4 (0.1)
21:0	0.3 (0.3)	0.2 (0.1)	0.6 (0.4)	0.3 (0.3)	0.4 (0.5)	tr	0.3 (0.4)	tr	0.2 (0.2)	0.3 (0.2)	0.3 (0)	tr
22:0	0.5 (0.2)	0.8 (0.1)	0.8 (0.3)	0.6 (0.2)	0.5 (0.1)	0.5 (0.1)	0.5 (0.4)	1.2 (0.1)	1.0 (0.1)	1 (0.3)	1.2 (0.3)	1.2 (0.1)
24:0	0.3 (0)	0.7 (0.3)	0.5 (0.2)	0.9 (0.2)	0.4 (0.2)	0.6 (0.1)	0.7 (0.5)	1.7 (0.1)	1.1 (0.3)	1.5 (0.4)	1.5 (0.3)	1.5 (0.3)
25:0	nd	nd	nd	nd	nd	nd	nd	0.3 (0.0)	0.2 (0.0)	0.2 (0.1)	0.3 (0.1)	0.8 (1.3)
ΣSFA	64.5 (15.2)	65.8 (9.5)	84.4 (14.2)	69.3 (14.2)	57.4 (6.7)	49.5 (6.9)	56.9 (15.7)	93.1 (2.6)	90.4 (5.4)	88.4 (10.1)	82.5 (11.3)	92.8 (2.6)
14:1ω5	nd	nd	nd	nd	nd	nd	nd	tr	0.2 (0.2)	0.2 (0.1)	tr	0.2 (0.2)
15:1ω1	nd	nd	nd	nd	nd	nd	nd	0.3 (0.7)	1.0 (1.4)	1.1 (0.6)	0.6 (0.5)	0.7 (0.8)
16:1ω5	1.1 (0.5)	0.6 (0.3)	0.3 (0.3)	0.4 (0.2)	1.2 (0.2)	0.8 (0.1)	0.3 (0.2)	nd	nd	nd	nd	nd
16:1ω7	7.8 (3.3)	6.9 (1.6)	4 (5.4)	6.6 (4.6)	9.4 (1.6)	12 (1.2)	18.3 (7.8)	0.4 (0.3)	0.4 (0.4)	0.6 (0.7)	0.9 (0.6)	tr
16:1ω9	0.7 (0.2)	1.7 (0.5)	0.4 (0.5)	1.9 (1.2)	0.9 (0.1)	1.2 (0.4)	0.9 (0.5)	0.3 (0.1)	0.3 (0.1)	0.6 (0.9)	1.2 (1)	0.3 (0.2)
17:1ω7	0.2 (0.1)	0.2 (0.1)	tr	0.2 (0.2)	0.2 (0.1)	0.2 (0.1)	tr	nd	nd	tr	nd	nd
17:1ω9	tr	tr	tr	tr	tr	tr	tr	tr	0.2 (0.1)	0.2 (0.1)	tr	tr
18:1ω5	tr	0.3 (0.2)	0.2 (0.2)	0.3 (0.1)	0.2 (0)	0.3 (0.1)	tr	tr	tr	tr	0.3 (0.2)	tr
18:1ω7	1.9 (0.7)	2.2 (0.6)	1 (1.3)	1.4 (0.7)	3 (1.1)	2.5 (0.9)	2.4 (1)	0.2 (0.2)	0.4 (0.3)	0.5 (0.6)	1.1 (0.4)	0.3 (0.5)
18:1ω9	7.1 (2.7)	6.7 (2)	1.9 (2.7)	6.2 (4.1)	9.7 (2.2)	6.4 (0.9)	6 (2.1)	0.7 (0.8)	2.9 (4.8)	3.2 (6.2)	7.3 (8)	0.5 (1)
20:1ω7	0.3 (0.3)	tr	tr	0.2 (0.1)	0.5 (0.3)	0.8 (0.6)	tr	tr	0.4 (0.4)	0.3 (0.2)	0.5 (0.2)	nd
20:1ω9	0.3 (0.2)	0.2 (0.1)	nd	tr	tr	0.2 (0.1)	tr	0.8 (1.4)	0.5 (0.8)	0.2 (0.3)	0.2 (0.2)	0.2 (0.3)
22:1ω9	tr	tr	tr	tr	tr	0.3 (0.1)	tr	nd	nd	tr	tr	nd
22:1 11	0.4 (0.3)	tr	tr	tr	0.4 (0.3)	0.7 (0.5)	tr	nd	nd	0.5 (0.8)	0.2 (0.1)	nd
ΣMUFA	20.1 (7)	19.4 (4.9)	8 (10.9)	17.9 (10.3)	26 (4.4)	25.6 (1.6)	28.6 (10.7)	3.2 (1.4)	6.2 (5.2)	8 (8.5)	13.1 (10.3)	2.8 (2.3)
16:2ω4	tr	tr	tr	tr	tr	0.4 (0.1)	0.3 (0.2)	nd	nd	nd	nd	nd
16:2ω6	tr	tr	tr	tr	tr	tr	0.2 (0.3)	nd	nd	nd	nd	nd
16:3ω3	tr	tr	nd	tr	nd	0.3 (0.2)	0.2 (0.2)	nd	nd	nd	nd	nd
16:4ω1	tr	0.2 (0.1)	tr	0.4 (0.2)	tr	1.1 (0.5)	0.6 (0.3)	nd	nd	nd	nd	nd
16:4ω3	0.6 (0.3)	0.4 (0.2)	0.2 (0.2)	0.4 (0.1)	0.6 (0.1)	0.7 (0.2)	0.4 (0.3)	nd	nd	nd	nd	nd
18:2ω6	1.3 (0.8)	1.9 (0.7)	0.5 (0.8)	2.8 (1.4)	1.9 (0.4)	2.6 (0.3)	2 (0.9)	tr	0.3 (0.4)	0.5 (0.9)	1.1 (1.3)	tr
18:3ω3	0.9 (0.7)	0.6 (0.2)	0.3 (0.5)	0.7 (0.2)	1.2 (0.3)	0.8 (0.1)	0.5 (0.3)	tr	tr	0.2 (0.1)	0.2 (0.1)	tr
18:4ω3	1.7 (1.4)	1.3 (0.4)	0.3 (0.5)	0.7 (0.3)	1.9 (0.6)	2.4 (0.2)	0.5 (0.4)	nd	nd	tr	nd	nd

Table 2 (continued)

FA	August							May				
	Pass Hytten		Basalt Island		Kap Breusing		SOM	Pass Hytten		Basalt Island		SOM
	s-POM	b-POM	s-POM	b-POM	s-POM	b-POM		s-POM	b-POM	s-POM	b-POM	
	n = 5	n = 5	n = 5	n = 4	n = 5	n = 4	n = 10	n = 4	n = 4	n = 5	n = 5	n = 9
20:4ω6	tr	tr	nd	tr	nd	tr	0.2 (0.2)	nd	nd	tr	nd	nd
20:5ω3	2.6 (2.2)	3.7 (2.1)	0.7 (1)	2.7 (2.5)	2.7 (1)	9 (4.9)	6.2 (3.3)	nd	nd	tr	nd	nd
22:2ω9	tr	tr	0.4 (0.5)	0.3 (0.3)	tr	0.2 (0.1)	0.5 (0.4)	nd	nd	nd	nd	nd
22:5ω3	tr	0.3 (0.2)	nd	0.5 (0.2)	tr	0.4 (0.1)	0.3 (0.6)	nd	nd	tr	nd	nd
22:6ω3	3.7 (3.5)	2.4 (1.3)	0.6 (0.9)	0.9 (0.6)	4 (1.4)	3.6 (0.9)	0.8 (0.7)	tr	nd	tr	tr	tr
ΣPUFA	11.6 (9.2)	11.4 (5)	3.1 (4)	9.7 (5.1)	13 (3.9)	22.1 (6.7)	12.9 (5.9)	0.2 (0.1)	0.3 (0.4)	1.1 (1.6)	1.5 (1.5)	tr
ΣBrFA	3.8 (0.7)	3.4 (0.4)	4.5 (0.6)	3.2 (0.9)	3.6 (0.5)	2.8 (0.6)	1.6 (0.5)	3.5 (1.9)	3.1 (1.2)	2.5 (0.2)	2.9 (0.9)	4.2 (1)
ΣPUFA/ΣSFA	0.2 (0.3)	0.2 (0.1)	0.0 (0.1)	0.2 (0.1)	0.2 (0.1)	0.5 (0.2)	0.3 (0.2)	0.0 (0.0)	0.0 (0.0)	0.0 (0.0)	0.0 (0.0)	0.0 (0.0)
ΣEFA	6.4 (5.7)	6.2 (3.4)	1.2 (1.9)	3.6 (3.1)	6.8 (2.4)	12.7 (5.8)	7.2 (3.9)	tr	nd	tr	tr	tr
16:1ω7/16:0	0.3 (0.2)	0.2 (0.1)	0.1 (0.2)	0.2 (0.2)	0.3 (0.1)	0.5 (0.1)	0.6 (0.3)	0.0 (0.0)	0.0 (0.0)	0.0 (0.0)	0.0 (0.0)	0.0 (0.0)
[FA] (mg g^{-1})	8.0 (2.1)	9.5 (5.0)	2.6 (0.9)	11.3 (4.4)	9.4 (2.3)	7.2 (5.7)	0.7 (0.4)	3.9 (0.5)	4.9 (2.5)	5.8 (2.4)	8.4 (4.4)	0.2 (0.0)

Table 3. Result of the 2-way permutational multivariate analysis of variance (PERMANOVA) realized on the fatty acid composition of summer and winter particulate organic matter samples based on the Bray-Curtis dissimilarity matrix. Site (*S*) and depth (*D*) are tested as fixed factors. Significant p-values are displayed in **bold**

Source of variation	df	MS	*F* Model	R^2	p-value
Summer					
Site (*S*)	2	0.1360	5.7102	0.2809	**0.0014**
Depth (*D*)	1	0.1327	5.5725	0.1371	**0.0052**
S × *D*	2	0.0198	0.8324	0.0410	0.5088
Residuals	22	0.0238		0.5411	
Winter					
Site (*S*)	1	0.0494	4.7766	0.2137	**0.0014**
Depth (*D*)	1	0.0251	2.4328	0.1088	**0.0494**
S × *D*	1	0.0222	2.1470	0.0960	0.0766
Residuals	13	0.0103		0.5815	

Breusing had a distinct FA composition, with high PUFA and monounsaturated FA (MUFA) proportions (22.1 and 25.6%, respectively; Table 2). This was particularly clear with FAs 20:5ω3 and 16:1ω7 reaching 9 and 12% in Kap Breusing, respectively, whereas they were less than 3.7 and 6.9% at the other 2 sites, respectively (Table 2). However, we did not observe any difference in FA concentration among stations ($p > 0.05$).

In May, the FA profiles differed significantly according to both site and depth ($p < 0.05$; Table 2) without any interaction between these 2 factors ($p = 0.077$). At both stations, POM appeared to be slightly more degraded in surface vs. bottom waters, as shown by the higher proportion of SFAs in s-POM (Table 2). Considering spatial variability, a higher proportion of ΣSFA was observed in Pass Hytten than in Basalt Island (93.1 vs. 88.4 for s-POM and 90.4 vs. 82.5 for b-POM, respectively; Table 2). However, such depth and station differences were relatively weak, as attested by the strong similarity between the s-POM and b-POM (84.7% similarity) as well as the Basalt Island and Pass Hytten samples (81.7% similarity).

3.1.2. SOM

SOM exhibited strong seasonal differences with much higher proportions of SFAs in May; yet these FAs represented only the half of the summer composition (ΣSFA = 92.2% vs. 56.9% for winter and summer, respectively). Similarly, only trace amounts of PUFAs were detected in May while their proportion reached 12.9% in August (Table 2). Summer PUFA and MUFA proportions were mainly linked to 20:5ω3 and 16:1ω7 contributions (18.3 and 6.2%, respectively; Table 2). Strong seasonal differences were also observed in the FA concentrations, which were 3-fold more abundant during August (0.7 vs. 0.2 for August and May, respectively, Table 2). In contrast with the POM samples, no differences among stations were observed in SOM during August ($p = 0.066$) and May ($p = 0.168$).

3.2. Stable isotopes of POM and SOM samples

In August, depth appeared to be the first discriminating factor in δ^{13}C and δ^{15}N values among the POM samples. At each station, these δ^{13}C and δ^{15}N values differed significantly between surface and bottom waters ($p < 0.0001$), with overall more enriched values by 1‰ for δ^{13}C and 2‰ for δ^{15}N in b-POM (Fig. 2). Globally, the isotopic signatures were closer between samples for the surface compared to the bottom stations. Moreover, no significant differences were observed between s-POM samples from Kap Breusing and Pass Hytten (for both δ^{13}C and δ^{15}N values) and between b-POM samples from Pass Hytten and Kap Breusing (only for δ^{15}N values, $p > 0.05$).

In contrast, all isotopic ratios associated with the May samples increased an average of 1.2 and 2.4‰ for δ^{13}C and δ^{15}N, respectively. These ratios did not vary significantly with depth within each station ($p > 0.05$; Fig. 2), but for both s-POM and b-POM, they differed significantly between stations ($p < 0.05$; Fig. 2).

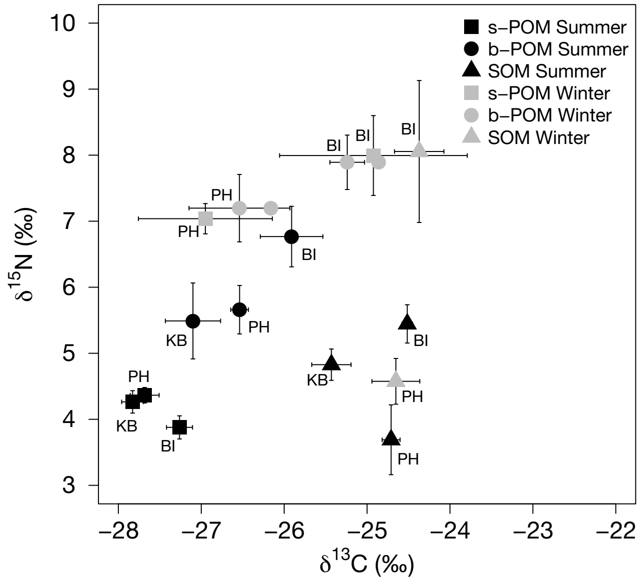

Fig. 2. Mean (±SD) δ^{13}C and δ^{15}N values of surface particulate organic matter (s-POM), bottom POM (b-POM), and sedimentary organic matter (SOM) from Pass Hytten (PH), Basalt Island (BI), and Kap Breusing (KB) collected during summer and winter

During summer, mean SOM δ^{13}C levels were more enriched, by 2.7 and 1.6‰, when compared to s-POM and b-POM, respectively (Fig. 2). Spatial differences were also observed during this season, but they were not significant between Pass Hytten and Basalt Island for δ^{13}C values and between Basalt Island and Kap Breusing for δ^{15}N values (pairwise test: $p > 0.05$). During May, the δ^{13}C level did not differ between Pass Hytten and Basalt Island ($p = 0.197$), and this level was also similar to that from August (−24.7‰ on average for SOM from Pass Hytten and Basalt Island during both seasons, $p > 0.05$; Fig. 2). δ^{15}N values differed significantly between Pass Hytten and Basalt Island ($p < 0.001$) and increased when compared to August levels by 0.9 and 2.6‰ for Pass Hytten and Basalt Island, respectively (Fig. 2).

3.3. FA profiles and isotope values of bivalves

3.3.1. FAs

FA signatures associated with the muscle and digestive gland samples of *Mya truncata* differed between seasons ($p < 0.01$; Tables 3 & 4). For the muscle samples, such differences were mainly attributable to variations in essential FAs (EFAs) (41.7 vs. 35.1% for August and May, respectively; Table 4). Temporal differences in the digestive gland data were especially obvious for the 20:5ω3/22:6ω3 ratio (14.5 vs. 1.3 in August and May, respectively; Table 4) and for 16:1ω7 (22.5 vs. 3.4% in August and May, respectively; Table 4). Interestingly, although FA profiles of muscles differed from those of digestives glands during August ($p < 0.01$, Table 5), they were not statistically different during May ($p = 0.322$; Table 5).

For *Astarte moerchi* tissues, both muscles and digestive glands had distinct FA profiles between seasons ($p < 0.001$; Table 5). The highest PUFA and EFA percentages for digestive glands were found in May (Table 4). In contrast, MUFAs were dominant during August, mainly due to values of 16:1ω7 that were twice as high compared to May (Table 4). A similar trend was observed for muscle FA profiles, with May contributions of EFAs and PUFAs double those of August (e.g. 5-fold higher in May for 22:6ω3: 14.5 vs. 2.8%; Table 4).

Table 4. Fatty acid (FA) composition of digestive gland (DG) and muscle (Mu) tissues of *Astarte moerchi* and *Mya truncata* collected from Basalt Island and Daneborg during summer (August) and winter (May). SFA: saturated FA; MUFA: monounsaturated FA; NMI: non-methylene-interrupted; PUFA: polyunsaturated FA; BrFA: branched FA; EFA: essential FA; EPA/DHA: 20:5ω3/22:6ω3; nd: not detected; tr: trace (FA percentage <0.2%). Standard deviations are represented within brackets. FAs with percentages lower than 1% in all samples are not included in this table. Winter FA compositions of digestive glands and muscles from *A. moerchi* originated from De Cesare (2016) and De Cesare et al. (2017)

FA	*Mya truncata*				*Astarte moerchi*			
	Basalt Island				Daneborg		Basalt Island	
	August		May		August		May	
	DG n = 5	Mu n = 5	DG n = 4	Mu n = 5	DG n = 10	Mu n = 6	DG n = 5	Mu n = 4
14:0	2.7 (0.6)	0.9 (0.1)	1.1 (0.4)	1.2 (0.1)	2.5 (0.7)	1.7 (0.7)	2.4 (0.4)	0.7 (0.2)
16:0	14.7 (0.5)	13.5 (1.1)	12.1 (2.9)	13.7 (1.2)	10.4 (0.4)	21.9 (5.8)	11.5 (1.3)	16.1 (1.5)
17:0	0.3 (0)	0.5 (0)	0.6 (0.1)	0.6 (0.1)	0.3 (0.1)	1.2 (0.4)	0.5 (0.1)	1.3 (0.1)
18:0	2.3 (0.5)	5.9 (1)	6.1 (1.7)	6.6 (1.7)	1.2 (0.4)	15.6 (11.2)	1.7 (0.6)	4.7 (0.5)
ΣSFA	20.3 (0.7)	21.3 (1.3)	20.7 (3.3)	22.8 (2.7)	14.6 (0.5)	42 (18.8)	16.6 (1.8)	23.3 (2.3)
16:1ω5	0.4 (0)	tr	tr	tr	1.6 (0.4)	1.1 (0.3)	1.2 (0.2)	0.3 (0)
16:1ω7	22.5 (4.3)	5.4 (0.8)	3.4 (1)	4.5 (0.8)	22.6 (5.5)	11.9 (4.5)	12.7 (3.2)	3.6 (0.8)
18:1ω5	0.5 (0.1)	0.3 (0)	0.4 (0)	0.3 (0.1)	4.5 (0.5)	5.5 (1.9)	4.6 (0.6)	5.7 (0.5)
18:1ω7	6.9 (0.7)	2.5 (0.2)	2 (0.6)	2.1 (0.4)	6.9 (1)	5.3 (1.8)	5.6 (0.5)	3.7 (0.5)
18:1ω9	0.8 (0.3)	2.6 (0.4)	2.6 (1.3)	2.9 (0.3)	1.3 (0.1)	2.9 (0.8)	2 (0.3)	2.3 (0.2)
20:1	1.7 (0.7)	6.9 (0.4)	nd	nd	1.3 (0.4)	1 (0.8)	nd	nd
20:1ω11	nd	nd	2.2 (0.4)	2.2 (0.4)	1.5 (0.8)	1 (0.7)	2.3 (0.6)	2.2 (0.2)
20:1ω7	1.7 (0.8)	3.5 (0.4)	5.1 (0.9)	4.1 (0.3)	2.9 (0.9)	3 (1.2)	3 (0.4)	3.7 (0.3)
20:1ω9	nd	nd	2.8 (0.4)	4.9 (0.8)	0.4 (0.2)	0.2 (0.2)	0.7 (0.2)	0.4 (0.1)
22:1ω9	nd	nd	2.3 (3.7)	0.4 (0.5)	tr	nd	0.4 (0.2)	0.3 (0.2)
ΣMUFA	35 (3.9)	21.5 (1.3)	22.1 (5.8)	23.3 (0.7)	43.6 (2.4)	32.2 (9.7)	33.2 (2.2)	22.6 (1.8)
18:4ω3	1.4 (0.2)	0.8 (0.4)	2.7 (1.2)	2.8 (1.2)	1.4 (0.3)	0.6 (0.6)	1.2 (0.1)	0.7 (0.4)
20:2 NMI	1 (0.7)	5.9 (0.8)	8.8 (3)	7.5 (2.7)	0.3 (0.1)	tr	0.2 (0.1)	tr
20:2ω9	nd	nd	nd	nd	1.1 (0.6)	1.1 (0.6)	1.3 (0.4)	2.5 (0.8)
20:4ω6	0.7 (0.2)	2.7 (0.2)	3.5 (0.5)	2.9 (0.2)	1.2 (0.9)	1.9 (1.1)	1.8 (0.3)	5.8 (0.5)
20:5ω3	32 (2.2)	22.4 (1)	17.8 (6.9)	17 (2.8)	25.9 (1.1)	12.5 (6.1)	29.5 (1.9)	17.8 (1.6)
21:5ω3	0.8 (0.2)	1.2 (0.2)	0.9 (0.6)	1.2 (0.3)	0.6 (0)	0.4 (0.4)	0.7 (0.1)	1 (0.1)
22:2ω6	tr	0.4 (0.1)	tr	tr	1.2 (0.5)	0.7 (0.6)	1.4 (0.4)	1.8 (0.2)
22:2ω9	tr	0.6 (0.1)	0.2 (0.3)	0.3 (0.2)	0.7 (0.4)	0.5 (0.4)	1 (0.3)	1.2 (0.3)
22:4ω6	tr	1.5 (0.3)	3.5 (1.6)	2.1 (0.3)	nd	nd	0.3 (0.1)	0.4 (0.1)
22:5ω3	tr	2 (1.1)	2.2 (0.6)	2.9 (0.5)	0.6 (0.4)	0.7 (0.9)	1 (0.2)	4.1 (0.7)
22:5ω6	tr	0.4 (0.1)	0.9 (0.5)	0.8 (0.5)	tr	1 (1.3)	0.3 (0.1)	0.8 (0.4)
22:6ω3	3.4 (2.4)	16.6 (1.3)	13.8 (2.6)	13.8 (1.5)	3.2 (0.5)	2.8 (2)	6.7 (1.6)	14.5 (1.9)
ΣPUFA	44.5 (4.1)	56.2 (1.6)	55.9 (6.6)	52.7 (3.2)	41.1 (2.4)	24.1 (11.3)	49.3 (1.1)	52.7 (3.9)
ΣBrFA	0.3 (0.1)	1 (0.1)	1.3 (0.5)	1.1 (0.3)	0.6 (0.2)	1.7 (1.1)	0.9 (0.2)	1.4 (0.2)
ΣEFA	36.1 (4)	41.7 (2.2)	35.1 (8.4)	33.8 (2.7)	30.3 (1.4)	17.2 (8.7)	38 (0.6)	38 (3.2)
ΣPUFA/ΣSFA	2.2 (0.2)	2.7 (0.2)	2.8 (0.6)	2.4 (0.5)	2.8 (0.2)	0.8 (0.6)	3 (0.3)	2.3 (0.4)
EPA/DHA	14.5 (10.9)	1.4 (0.1)	1.3 (0.4)	1.3 (0.3)	8.4 (1.4)	5 (1.2)	4.7 (1.7)	1.2 (0.2)
[FA] mg g^{-1}	NA	NA	21.9 (21.1)	4.5 (2.4)	123.4 (48.3)	19.9 (7.5)	51.8 (24.5)	3.9 (0.4)

3.3.2. Isotopes

Although isotopic signatures of the digestive glands of *A. moerchi* ($\delta^{13}C$ = −24.2‰ and $\delta^{15}N$ = 6.5‰) and *M. truncata* ($\delta^{13}C$ = −24.7‰ and $\delta^{15}N$ = 6.2‰) were similar during August, they were more distinct in May (Fig. 3). In fact, seasonal differences for $\delta^{13}C$ and $\delta^{15}N$ were observed in *M. truncata* (+3 and +1.5‰ between August and May for $\delta^{13}C$ and $\delta^{15}N$, respectively; $p < 0.05$; Fig. 3) but not in *A. moerchi* (+0.4 and −0.2‰ between August and May for $\delta^{13}C$ and $\delta^{15}N$, respectively; $p > 0.05$; Fig. 3). Regarding muscle tissues, no seasonal variations of $\delta^{13}C$ and $\delta^{15}N$ were observed in either species (Fig. 3), and no inter-specific variations were observed during each season ($p > 0.05$).

In May, $\delta^{13}C$ and $\delta^{15}N$ values of s-POM, b-POM, and macroalgae samples clearly differed from those of digestive gland and muscle tissues in both bivalves (Fig. 3B). In contrast, isotopic values of *A. moerchi* and *M. truncata* became closer in summertime to POM and SOM values (Fig. 3A).

Table 5. Result of the 1-way permutational multivariate analyses of variance (PERMANOVA). The upper part relates to the fatty acid composition of digestive gland (DG) and muscle (Mu) tissues of *Astarte moerchi* and *Mya truncata*, with season as a fixed factor. The lower part relates to the fatty acid composition of *A. moerchi* and *M. truncata* from summer (Aug) and winter (May) seasons, with tissue as a fixed factor. Significant p-values are displayed in **bold**

Tested group	df	MS	*F* model	R^2	p-value
Season as fixed factor					
M. truncata DG	1	0.4866	36.8920	0.8405	**0.0062**
M. truncata Mu	1	0.0931	20.9360	0.7235	**0.0074**
A. moerchi DG	2	0.1092	16.6220	0.6129	**0.0001**
A. moerchi Mu	2	0.2220	7.2209	0.4593	**0.0005**
Tissue as fixed factor					
M. truncata May	1	0.0166	1.175	0.1437	0.3220
M. truncata Aug	1	0.3589	99.035	0.9253	**0.0084**
A. moerchi May	1	0.3243	48.958	0.7776	**0.0001**
A. moerchi Aug	1	0.4510	19.831	0.5862	**0.0001**

4. DISCUSSION

4.1. Influences of seasonal and spatial constraints on POM and SOM patterns

4.1.1. Seasonal patterns

There have been few studies of the seasonal variability between ice cover and open sea periods in the main pelagic and benthic food sources of bivalves in High Arctic coastal areas (but see Connelly et al. 2015, 2016). This work constitutes the first contribution for the Young Sound fjord. During the productive summer period, FA composition of the POM in bottom waters revealed the dominant contribution of several photosynthetic producers, such as diatoms (16:1ω7, 20:5ω3), dinoflagellates (18:4ω3, 22:6ω3), and macroalgae (18:2ω6, 18:3ω3, 18:4ω3, 20:5ω3). Moreover, relatively high summer abundances of essential FAs (e.g. 20:5ω3, 22:6ω3, 18:4ω3) in animals and bivalves contrast with the winter situation. In winter, with the absence of *in situ* primary production, POM was highly degraded; this was reflected by the large proportion of total SFAs (Rhead et al. 1971, Connelly et al. 2015, 2016). Very low levels of total PUFAs during May (i.e. <1.5%) indicate that the extended duration of ice and snow cover in Young Sound is paired with the absence of fresh organic matter for primary consumers compared to other Arctic fjords (e.g. ΣPUFA = 14.3–39.8% in Kongsfjorden, 13.4% in Rijpfjorden; Leu et al. 2006, 2011). In fact, in May, after 4–5 mo in darkness, the POM lipid concentrations measured in Young Sound (2.6–11.3 mg g^{-1}) were much lower than in any other Arctic fjord (for example, 95.4–98.6 mg g^{-1} in Kobbefjord; Gaillard et al. 2017). In May, despite 24 h of daylight, the presence of snow on the sea ice prevents the transmission of light (Glud et al. 2007), and primary production does not start before mid-July when melt-water ponds that form on the sea ice intensify light transmission. This in turn triggers a short algal bloom (Rysgaard et al. 1999). Photosynthetically active radiation (PAR) sensors fixed at 1 m depth below the sea ice revealed no available PAR for primary producers in May (M. K. Sejr unpubl. data). For SOM, seasonal changes in FA composition show the same trends as in May POM, as shown by low FA

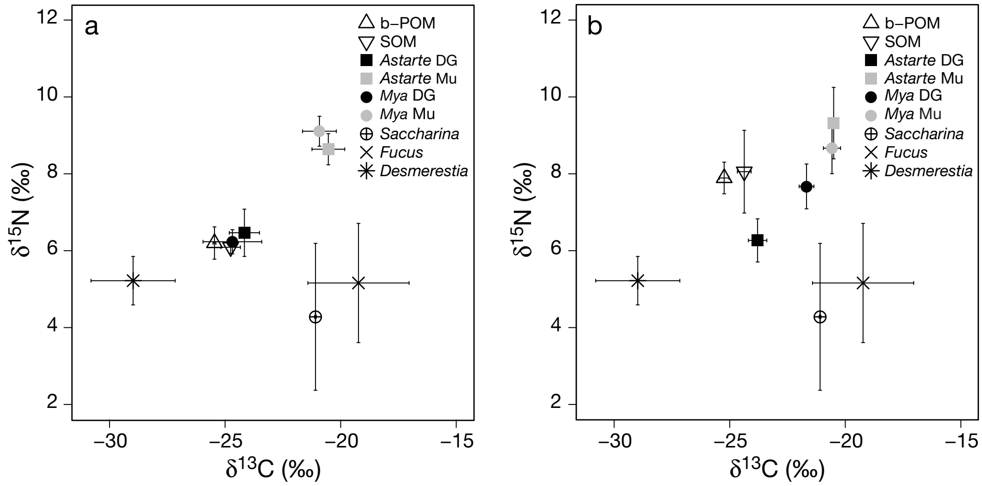

Fig. 3. Mean (±SD) $\delta^{13}C$ and $\delta^{15}N$ values of *Astarte moerchi* and *Mya truncata* tissues and their potential food sources during (A) summer and (B) winter. b-POM: bottom-particulate organic matter; SOM: sedimentary organic matter; DG: digestive gland; Mu: muscle. Stable isotope values from macroalgae (*Saccharina*, *Fucus*, and *Desmerestia*) and b-POM, SOM, and *Astarte*'s tissues from wintertime originated from De Cesare (2016) and De Cesare et al. (2017)

and total PUFA concentrations. In contrast, diatoms dominate the SOM during the summer, as revealed by higher relative proportions of 16:1ω7 and 20:5ω3, whereas dinoflagellates (18:4ω3, 22:6ω3) and macroalgae markers (18:2ω6, 18:3ω3, 20:4ω6, 20:5ω3) suggest additional contributions of these primary sources to the pool of organic matter.

The absence of significant primary production in May was confirmed by a general increase in δ^{15}N in both POM and SOM. Indeed, food webs from sea ice-covered ecosystems switch to heterotrophy during the polar night due to the development of protozoans and/or microbial planktonic communities (Berge et al. 2015). As heterotrophic microorganisms may be consumers of organic matter, their isotopic signatures should be enriched in δ^{15}N compared to autotrophic algae (Hoch et al. 1996, Tamelander et al. 2009). Hence, such δ^{15}N enrichment could explain the seasonal increase of the δ^{15}N in POM during winter (Tamelander et al. 2009, Kędra et al. 2012), but it also may reflect the increased contribution of animal detritus and fecal pellets (Sampei et al. 2012) and diagenesis (Schulz & Zabel 2006).

4.1.2. Spatial patterns

The Marine Basis Monitoring Program has conducted annual surveys in August since 2003 that document the strong influence of terrestrial runoff on the water column, especially in surface waters (above 10 m depth), as attested by lower salinity and higher turbidity measurements (Citterio et al. 2017, Middelbo et al. 2018). This influence of direct freshwater inputs is confirmed by s-POM δ^{15}N values (4.2 ± 0.3‰), which are almost identical with riverine δ^{15}N values (4.3 ± 0.3‰, Zackenberg River; Rysgaard & Sejr 2007). Poorer organic matter quality in s-POM compared to b-POM (as expressed by the high levels of ΣSFA and low levels of ΣPUFA) suggests an increase in the relative proportion of detrital particles compared to living cells in surface waters (Leu et al. 2006, Mayzaud et al. 2013). Such observations are likely explained by the inflow of nutrient-depleted freshwater (confined to surface waters), which may both discharge a huge amount of terrestrial detrital particles and decrease primary productivity (Mayzaud et al. 2013, Meire et al. 2016, 2017). This hypothesis is consistent with previous findings in Young Sound, which showed lower chlorophyll *a* (chl *a*) concentrations in the most runoff-exposed parts of the fjord (Meire et al. 2016, Arendt et al. 2016, Middelbo et al. 2018).

Overall, POM from Young Sound bottom waters was nutritionally richer than that from surface waters, as reflected by higher proportions of EFAs. However, the related δ^{13}C and δ^{15}N values were highly variable among the stations, and we hypothesize that this could be attributable to their differential exposure to freshwater inputs. Thus, higher δ^{13}C and δ^{15}N found in b-POM in Pass Hytten and Basalt Island could be explained by greater exposure of inner fjord waters to nutrient-depleted and CO_2-desaturated freshwater inputs (Tamelander et al. 2009, Meire et al. 2015, 2016). It also possibly indicates more degraded organic matter at the inner stations due to higher bacterial activity (McTigue et al. 2015). These spatial SI discrepancies may also reflect different bloom dynamics (duration, kinetics) among stations, since isotopic signatures generally show an enrichment during a bloom (Savoye et al. 2003, Tamelander et al. 2009). In addition, the higher percentages of diatom and dinoflagellate markers (see above details) in Kap Breusing may reflect local primary productivity that is higher in the outer than in the inner part of the fjord. Accordingly, Meire et al. (2016) showed that upwelling of nitrate and phosphate-rich waters around the fjord's mouth sustains a high phytoplankton biomass throughout the summer.

Identifying and quantifying the sources of organic matter in superficial marine sediments is a difficult task, as terrestrial inputs, benthic primary producers (including microphytobenthos and macroalgae), and sedimentation of POM may all be present. For instance, SOM quality and quantity may be affected by benthic organisms through bioturbation, burrowing, use of organic matter, and excretion (e.g. Glud et al. 2000). Although FA analysis results show an input of macroalgae to the SOM, their contributions should be rather limited. Indeed, previous compound-specific isotopic analyses excluded the contribution of *Desmarestia aculeata* to the pelagic and benthic pool of organic matter (De Cesare et al. 2017, G. Bridier unpubl. data). In addition, the *Fucus* sp. and *Saccharina latissima* contributions seem relatively weak, as δ^{13}C values of both species (19.2 ± 2.2 and −21.1 ± 0.0‰, respectively) strongly differ from the SOM δ^{13}C value (−24.9 ± 0.6‰). According to published δ^{13}C signatures of Arctic microphytobenthos (from −23.9 to −20.0‰; Oxtoby et al. 2016), riverine POM (−25.6 ± 0.1‰, Zackenberg River; Rysgaard & Sejr 2007), and b-POM measured in the present study (−26.5 ± 0.6‰), the SOM δ^{13}C values probably reflect either (1) a strong contribution of terrestrial organic matter associated with a minor contribution of microphytobenthos, or (2) an equal contribution of marine b-POM and microphytobenthos to SOM. According to the C/N ratios calculated from the Young Sound (18.3 ± 1.7, 10.3 ± 0.2, and 9.1 ± 0.2 for the SOM of Pass Hytten, Basalt Island, and Kap Breusing, respectively) and riverine data (10 < C/N ratio < 40, Zackenberg river; Rysgaard & Sejr 2007), the FA composition of Kap Breusing sediment should be less influenced by terrestrial inputs than the other 2 sites. Moreover, FA profiles of Kap Breusing and Basalt Island sediments display the highest percentages of diatom markers (16:1ω7, 16:4ω1, and 20:5ω3), strongly suggesting that the associated SOM originates from both microphytobenthos and sedimented phytoplankton (second scenario). In contrast, sediments from Pass Hytten should receive organic matter from dominant terrestrial inputs with a low contribution from marine primary producers (first scenario).

Comparing marine and riverine POM and SOM δ^{13}C values, Rysgaard & Sejr (2007) estimated that half of the Young Sound's sediment organic carbon came from terrestrial sources. However, the marine POM δ^{13}C value (−21.6 ± 0.3‰) used for their estimate originates from a study conducted by Hobson & Welch (1992) in Barrow Strait (NE Canada) that differs from those found here (−26.5 ± 0.6‰, present study; −25.5 ± 0.1‰, De Cesare et al. 2017). Although Young Sound's POM δ^{13}C isotopic ratios may vary across years, multiannual values relative to a site close to Ny-Ålesund (Kongsfjorden, Svalbard) during May vary slightly between 2007, 2012, and 2013 (−21.6 ± 0.2, −22.7, and −23.1 ± 0.4‰, respectively; Renaud et al. 2011, De Cesare 2016, Calleja et al. 2017). We therefore suggest that differences in POM δ^{13}C values between Young Sound and Barrow Strait do not depend on temporal variations, and that future work on the contribution of terrestrial organic matter to SOM should be based on local POM δ^{13}C values.

4.2. Diet of *Astarte moerchi* and *Mya truncata*

Since sampling of bivalves was conducted over 2 different years, the seasonal comparison of FA profiles and SI signatures probably reflects both seasonal and interannual variabilities of their food sources. However, as the FA profiles of Arctic bivalves are usually more sensitive to seasonality than interannual variability (e.g. Birkely et al. 2003), we are confident that the FA profiles from a specific origin and season will be quite stable between years. Moreover, because of the huge seasonality of the Young Sound's physical environment and carbon transport (Rysgaard et al. 2003), the bivalves' food sources should also display much higher seasonal than interannual variations. In contrast, it is more difficult to distinguish seasonal from interannual variability in bivalves' SI signatures, since they vary minimally between seasons and years (Renaud et al. 2011, Kędra et al. 2012, McTigue & Dunton 2014, Gaillard et al. 2017). Thus, seasonal differences in bivalves' SI signatures should be interpreted with caution.

Usually, FAs associated with neutral lipids (used as energy storage) are directly mobilized from the diet, while polar FAs (cell membrane components) are subjected to strong physiological regulation (Jezyk & Penicnak 1966, Napolitano & Ackman 1992, Pazos et al. 2003, Gaillard et al. 2015). Since the digestive gland has a lipid storage function, this tissue displays high levels of neutral compared to polar lipids. In contrast, muscle tissue contains low levels of neutral and thus higher proportions of polar lipids (Napolitano & Ackman 1992, Pazos et al. 2003). For that reason, digestive glands usually have a higher lipid turnover rate and diet sensitivity, whereas muscles are more sensitive to physiological regulation (Napolitano & Ackman 1992, Napolitano et al. 1997, Nérot et al. 2015). Such inter-tissue differences were also evident in the present study; unlike digestive glands for which high levels of 20:5ω3 and 22:6ω3 are always associated with high levels of diatoms or dinoflagellates dietary FA markers, these 2 FAs were not associated with high levels of their dietary FA markers in muscle. Therefore, the selective retention of 20:5ω3 and 22:6ω3, which are 2 EFAs (Soudant et al. 1996, Parrish 2009), confirms that muscle and digestive glands may constitute real proxies of bivalves' diet and physiological conditions, respectively.

During summer, the FA compositions and isotopic signatures of the digestive glands of *Astarte moerchi* and *Mya truncata* were very similar. This suggests that both bivalves have the same diet dominated by diatoms, as shown by the high proportions of 16:1ω7 and 20:5ω3, which are also found in POM and SOM during summer (De Cesare et al. 2017). Such strong similarities in FA profiles between bivalves and their food sources indicate tight benthic–pelagic coupling as well as an efficient organic matter transfer from primary producers to primary consumers in the Young Sound food web. If we consider the summer FA composition of muscles, both species exhibit rather good physiological states as indicated by high levels of EFAs, as these are essential for somatic growth, reproduction, and the maintenance of cell membrane fluidity (Soudant et al. 1996, Parrish 2009).

During winter, $\delta^{13}C$ values associated with POM, SOM, and macroalgae sources were too distinct from those of digestive glands and muscles, thus these sources were unlikely to contribute to the bivalves' diet. Although macroalgae $\delta^{13}C$ values may slightly fluctuate between seasons (Vizzini & Mazzola 2003), the lack of macroalgal FA markers in bivalve tissues provides evidence that macroalgae were not consumed during winter. We thus suggest that poor trophic environmental winter conditions, evidenced by highly degraded organic matter sources, induce a drastic decrease and more likely an interruption in the feeding activity of both bivalves. Such winter quiescence has previously been observed in bivalves (Pernet et al. 2007, Comeau et al. 2012) but contrasts with numerous studies reporting the persistence of long-term 'food banks' in polar benthic ecosystems (e.g. Mincks et al. 2005) that fuel many organisms by labile detritus (McClintock 1994, Mincks et al. 2008, McMeans et al. 2015, Silberberger et al. 2018). This is not the case in Young Sound fjord, where the survival of *A. moerchi* and *M. truncata* individuals relates to their reliance on energetic reserves under a poor trophic winter environment. Moreover, each species displays a distinct pattern in its ability to use these lipids. Hence, the similar FA profiles observed during winter between digestive glands and muscle tissues of *M. truncata* may reflect a depletion of its lipid reserves. This phenomenon will induce a decrease in the concentration of neutral lipids (constituent of the lipid reserves in digestive glands) and will mechanically increase the proportion of polar lipids in this tissue (i.e. there will be a higher proportion of polar lipids in winter for a similar concentration between the 2 seasons). Hence, the similar lipid class composition between digestive glands and muscles may increase the similarity in their lipid profiles. The seasonal increase of digestive gland $\delta^{13}C$ values may strengthen this hypothesis, since lipids are more depleted in $\delta^{13}C$ than in other compounds (Lorrain et al. 2002). The increase in $\delta^{13}C$ and $\delta^{15}N$ may also reflect the impact of starvation on *M. truncata* metabolism (Hertz et al. 2015, Doi et al. 2017). A simultaneous percentage decrease in 20:5ω3 and 22:6ω3 with a percentage increase in 20:2 non-methylene-interrupted (NMI) FA also confirms the poor physiological state of *M. truncata* during winter. In fact, NMI biosynthesis should be critical for this species for maintaining both structure and fluidity of their cell membranes in the face of a decrease in PUFA levels (Pernet et al. 2007, Gaillard et al. 2015). The lipid reserves were less depleted in winter for *A. moerchi* than *M. truncata.* In fact, the winter FA concentration in digestive glands for *A. moerchi* was twice as high as for *M. truncata*, and the proportions of EFA and FA trophic markers remained high compared to those in summer. Such species-specific seasonal patterns of lipid reserves could be explained by (1) differential lipid mobilization during winter, or (2) the differential ability to build lipid reserves during the rise in primary production. Data from the present study do not support one hypothesis over the other. For instance, the first hypothesis may reflect the bivalves' ability to reduce their metabolic rate or their reproduction investment. However, both species showed a similar decrease in their ω3/ω6 ratio during winter, which may indicate that they devote similar efforts to reproduction (Leroy et al. 2013, De Cesare 2016). Likewise, little information is available about their ability to reduce their metabolic rate during starvation or any other physiological stress (e.g. Abele-Oeschger & Oeschger 1995, Camus et al. 2003). Hence, further studies, such as *in situ* measurements of bivalve metabolic rate or clearance rates during winter or observations about their ability to store lipid during a short food supply (e.g. as for *Yoldia hyperborea*; Stead et al. 2013), will be thus helpful to better explore such hypotheses.

Finally, about 30 % of Young Sound's seafloor is below 100 m depth (Rysgaard et al. 2003), and the link between filter feeders and primary producers in deeper basins may differ from our results from shallow areas. Although vertical carbon fluxes at both shallow and deeper depths have not been quantified in this fjord, the very low abundance of benthic macrofauna at 85 m depth (Glud et al. 2000, Sejr et al. 2000) suggests a decrease in carbon transfer to deeper areas via pelagic–benthic coupling (Ambrose & Renaud 1995). However, because similar C/N ratios were found at 20 and 163 m depth (Glud et al. 2000), we hypothesize that organic matter transfer from the surface to deeper basins would be fast enough to fuel benthic filter-feeding species with relatively fresh organic matter (i.e. similar to that in shallow waters). Such tight pelagic–benthic coupling has previously been reported up to 600 m depth in the High Arctic Canadian archipelago for the filter-feeding bivalve *Bathyarca glacialis* (Gaillard et al. 2015).

5. CONCLUSIONS AND OUTLOOK

Extremely long sea-ice cover deprives Young Sound of fresh primary production during most of the year, while freshwater inputs strongly degrade the quality of organic matter in surface waters and seems to control the primary production dynamics within bottom waters during summer. However, distinct adaptations are observed among filter-feeding bivalves that allow them to cope with the long winter conditions: *A. moerchi* seems to be best adapted to live on stored energy reserves, whereas the depletion of *M. truncata*'s lipid reserves during May suggest it has less energetic margin to survive the winter.

In the face of climate change, Young Sound will be exposed to a continued freshening of its surface water masses, preventing the renewal of deeper basin water masses in the inner fjord (e.g. Sejr et al. 2017, Boone et al. 2018). Numerous studies have highlighted the effect of such a freshening on the Young Sound's primary productivity through a decrease in light (Murray et al. 2015) and nutrient availability (Meire et al. 2016). Results from our study suggest that this decrease in primary productivity may be amplified by a decrease in organic matter quality in the inner parts of this fjord. In contrast, the outer part of Young Sound may be less affected by this freshening due to its sill, which allows nutrient replenishment through vertical mixing (Meire et al. 2016). However, such impoverishment of the trophic environment in the inner fjord may weaken the ability of some primary consumers (e.g. *Mya truncata*) to accumulate enough lipid reserves during summer to cope with winter conditions, and this might have cascading effects on their survival and renewal potential. Considering the key functional role of such filter-feeding bivalves for the transfer of organic matter toward higher trophic levels, such a shift could impact the entire benthic food web from primary producers to mammals, especially walruses, which can consume up to 57 kg of fresh *Mya truncata* d^{-1} (Born et al. 2003).

Acknowledgements. We are grateful to Erwan Amice for his difficult work in collecting bivalves and SOM samples while SCUBA diving. We greatly thank Najet Thiney for her valuable help in the laboratory of the Muséum National d'Histoire Naturelle (MNHN, Paris). Many thanks to S. De Cesare for sharing raw data from De Cesare et al. (2017) and De Cesare (2016). We are grateful to the Université de Bretagne Occidentale/LIA BeBEST and the 'Allocations de recherche doctorale' from the Brittany Region Council for co-funding the PhD thesis of G.B. Funding was provided by the Institut Polaire Francais Paul-Emile Victor (IPEV – PRIVARC project), the French 'Agence Nationale de la Recherche' (ANR ASTRID – GAAP project), the European H2020 INTAROS program and the Observatoire Marin de l'IUEM (UMS 3113). We acknowledge the support of the MarineBasis programme (part of the Greenland Ecosystem Monitoring) and of Zackenberg staff during the surveys, especially Egon Randa Frandsen and Henrik Spenggaard Munch. Two anonymous reviewers are thanked for their English corrections and relevant remarks, which greatly improved the manuscript.

LITERATURE CITED

Abele-Oeschger D, Oeschger R (1995) Hypoxia-induced autoxidation of haemoglobin in the benthic invertebrates *Arenicola marina* (Polychaeta) and *Astarte borealis* (Bivalvia) and the possible effects of sulphide. J Exp Mar Biol Ecol 187:63–80

AMAP (Arctic Monitoring and Assessment Programme) (2017) Snow, water, ice and permafrost in the Arctic (SWIPA). Arctic Monitoring and Assessment Programme (AMAP), Oslo

Ambrose WG, Renaud PE (1995) Benthic response to water column productivity patterns: evidence for benthic–pelagic coupling in the Northeast Water Polynya. J Geophys Res 100:4411–4421

Anderson MJ, Walsh DC (2013) PERMANOVA, ANOSIM, and the Mantel test in the face of heterogeneous dispersions: What null hypothesis are you testing? Ecol Monogr 83:557–574

Anderson MJ, Gorley RN, Clarke KR (2008) PERMANOVA+ for PRIMER: guide to software and statistical methods. Primer-E, Plymouth

Ardyna M, Babin M, Gosselin M, Devred E, Rainville L, Rainville L, Tremblay JÉ (2014) Recent Arctic Ocean sea ice loss triggers novel fall phytoplankton blooms. Geophys Res Lett 41:6207–6212

Arendt KE, Agersted MD, Sejr MK, Juul-Pedersen T (2016) Glacial meltwater influences on plankton community structure and the importance of top-down control (of primary production) in a NE Greenland fjord. Estuar Coast Shelf Sci 183:123–135

Arimitsu ML, Piatt JF, Mueter F (2016) Influence of glacier runoff on ecosystem structure in Gulf of Alaska fjords. Mar Ecol Prog Ser 560:19–40

Arrigo KR, van Dijken GL (2015) Continued increases in Arctic Ocean primary production. Prog Oceanogr 136: 60–70

Bamber J, van den Broeke M, Ettema J, Lenaerts J, Rignot E (2012) Recent large increases in freshwater fluxes from Greenland into the North Atlantic. Geophys Res Lett 39: L19501

Bendtsen J, Gustafsson K, Rysgaard S, Vang T (2007) Physical conditions, dynamics and model simulations during the ice-free period of the Young Sound/Tyrolerfjord system. Medd Gronl Biosci 58:45–59

Bendtsen J, Mortensen J, Rysgaard S (2014) Seasonal surface layer dynamics and sensitivity to runoff in a high Arctic fjord (Young Sound/Tyrolerfjord, 74°N). J Geophys Res Oceans 119:6461–6478

Berge J, Renaud PE, Darnis G, Cottier F and others (2015) In the dark: a review of ecosystem processes during the Arctic polar night. Prog Oceanogr 139:258–271

Birkely SR, Grahl-Nielsen O, Gulliksen B (2003) Temporal variations and anatomical distributions of fatty acids in the bivalve *Mya truncata*, L. 1758, from Isfjorden, Spitsbergen. Polar Biol 26:83–92

Bligh EG, Dyer WJ (1959) A rapid method of total lipid extraction and purification. Can J Biochem Physiol 37: 911–917

Boone W, Rysgaard S, Carlson DF, Meire L and others (2018) Coastal freshening prevents fjord bottom water renewal in Northeast Greenland: a mooring study from 2003 to 2015. Geophys Res Lett 45:2726–2733

Born EW, Rysgaard S, Ehlmé G, Sejr M, Acquarone M, Levermann N (2003) Underwater observations of foraging free-living Atlantic walruses (*Odobenus rosmarus rosmarus*) and estimates of their food consumption. Polar Biol 26:348–357

Calleja ML, Kerhervé P, Bourgeois S, Kędra M and others (2017) Effects of increase glacier discharge on phytoplankton bloom dynamics and pelagic geochemistry in a high Arctic fjord. Prog Oceanogr 159:195–210

Camus L, Birkely SR, Jones MB, Børseth JF and others (2003) Biomarker responses and PAH uptake in *Mya truncata* following exposure to oil-contaminated sediment in an Arctic fjord (Svalbard). Sci Total Environ 308: 221–234

Carmack E, Winsor P, Williams W (2015) The contiguous panarctic riverine coastal domain: a unifying concept. Prog Oceanogr 139:13–23

Citterio M, Sejr MK, Langen PL, Mottram RH and others (2017) Towards quantifying the glacial runoff signal in the freshwater input to Tyrolerfjord–Young Sound, NE Greenland. Ambio 46:146–159

Comeau LA, Mayrand É, Mallet A (2012) Winter quiescence and spring awakening of the Eastern oyster *Crassostrea virginica* at its northernmost distribution limit. Mar Biol 159:2269–2279

Connelly TL, McClelland JW, Crump BC, Kellogg CTE, Dunton KH (2015) Seasonal changes in quantity and composition of suspended particulate organic matter in lagoons of the Alaskan Beaufort Sea. Mar Ecol Prog Ser 527:31–45

Connelly TL, Businski TN, Deibel D, Parrish CC, Trela P (2016) Annual cycle and spatial trends in fatty acid composition of suspended particulate organic matter across the Beaufort Sea shelf. Estuar Coast Shelf Sci 181: 170–181

Dalsgaard J, John MS, Kattner G, Müller-Navarra D, Hagen W (2003) Fatty acid trophic markers in the pelagic marine environment. Adv Mar Biol 46:225–340

De Cesare S (2016) Les bivalves filtreurs *Astarte moerchi*: modèle biologique pour l'étude des écosystèmes marins arctiques. PhD dissertation, Muséum National d'Histoire Naturelle, Paris. https://tel.archives-ouvertes.fr/tel-01884169

De Cesare S, Meziane T, Chauvaud L, Richard J and others (2017) Dietary plasticity in the bivalve *Astarte moerchi* revealed by a multimarker study in two Arctic fjords. Mar Ecol Prog Ser 567:157–172

Doi H, Akamatsu F, Gonzales AL (2017) Starvation effects on nitrogen and carbon stable isotopes of animals: an insight from meta-analysis of fasting experiments. R Soc Open Sci 4:170633

Falk-Petersen S, Pavlov V, Timofeev S, Sargent JR (2007) Climate variability and possible effects on arctic food chains: the role of *Calanus*. In: Ørbæk JB, Tombre T, Kallenborn R, Hegseth E, Falk-Petersen S, Hoel AH (eds) Arctic alpine ecosystems and people in a changing environment. Springer-Verlag, Berlin, p 147–166

Fry B (2006) Stable isotope ecology. Springer, New York, NY

Gaillard B, Meziane T, Tremblay R, Archambault P, Layton KKS, Martel AL, Olivier F (2015) Dietary tracers in *Bathyarca glacialis* from contrasting trophic regions in the Canadian Arctic. Mar Ecol Prog Ser 536:175–186

Gaillard B, Meziane T, Tremblay R, Archambault P and others (2017) Food resources of the bivalve *Astarte elliptica* in a sub-Arctic fjord: a multi-biomarker approach. Mar Ecol Prog Ser 567:139–156

Glud RN, Risgaard-Petersen N, Thamdrup B, Fossing H, Rysgaard S (2000) Benthic carbon mineralization in a high-Arctic sound (Young Sound, NE Greenland). Mar Ecol Prog Ser 206:59–71

Glud RN, Rysgaard S, Kühl M, Hansen JW (2007) The sea ice in Young Sound: implications for carbon cycling. Medd Gronl Biosci 58:62–85

Hertz E, Trudel M, Cox MK, Mazumder A (2015) Effects of fasting and nutritional restriction on the isotopic ratios of nitrogen and carbon: a meta-analysis. Ecol Evol 5: 4829–4839

Hobson KA, Welch HE (1992) Determination of trophic relationships within a high Arctic marine food web using δ^{13}C and δ^{15}N analysis. Mar Ecol Prog Ser 84:9–18

Hoch MP, Snyder RA, Cifuentes LA, Coffin RB (1996) Stable isotope dynamics of nitrogen recycled during interactions among marine bacteria and protists. Mar Ecol Prog Ser 132:229–239

Iken K, Bluhm BA, Dunton K (2010) Benthic food-web structure under differing water mass properties in the southern Chukchi Sea. Deep Sea Res II 57:71–85

Jacob U, Mintenbeck K, Brey T, Knust R, Beyer K (2005) Stable isotope food web studies: a case for standardized sample treatment. Mar Ecol Prog Ser 287:251–253

Jezyk PF, Penicnak AJ (1966) Fatty acid relationships in an aquatic food chain. Lipids 1:427–429

Kędra M, Kuliński K, Walkusz W, Legeżyńska J (2012) The shallow benthic food web structure in the high Arctic does not follow seasonal changes in the surrounding environment. Estuar Coast Shelf Sci 114:183–191

Kędra M, Moritz C, Choy ES, David C and others (2015) Status and trends in the structure of Arctic benthic food webs. Polar Res 34:23775

Kelly JR, Scheibling RE (2012) Fatty acids as dietary tracers in benthic food webs. Mar Ecol Prog Ser 446:1–22

Kjeldsen KK, Korsgaard NJ, Bjørk AA, Khan SA and others (2015) Spatial and temporal distribution of mass loss from the Greenland ice sheet since AD 1900. Nature 528: 396–400

Kuliński K, Kędra M, Legeżyńska J, Gluchowska M, Zaborska A (2014) Particulate organic matter sinks and sources in high Arctic fjord. J Mar Syst 139:27–37

Kwok R, Rothrock DA (2009) Decline in Arctic sea ice thickness from submarine and ICESat records: 1958–2008. Geophys Res Lett 36:L15501

Lawson EC, Wadham JL, Tranter M, Stibal M and others (2014) Greenland Ice Sheet exports labile organic carbon to the Arctic oceans. Biogeosciences 11:4015–4028

Leroy F, Meziane T, Riera P, Comtet T (2013) Seasonal variations in maternal provisioning of *Crepidula fornicata* (Gastropoda): fatty acid composition of females, embryos and larvae. PLOS ONE 8:e75316

Leu E, Falk-Petersen S, Kwaśniewski S, Wulff A, Edvardsen K, Hessen DO (2006) Fatty acid dynamics during the spring bloom in a High Arctic fjord: importance of abiotic factors versus community changes. Can J Fish Aquat Sci 63:2760–2779

Leu E, Søreide JE, Hessen DO, Falk-Petersen S, Berge J (2011) Consequences of changing sea-ice cover for primary and secondary producers in the European Arctic shelf seas: timing, quantity, and quality. Prog Oceanogr 90:18–32

Lorrain A, Paulet YM, Chauvaud L, Savoye N, Donval A, Saout C (2002) Differential $\delta^{13}C$ and $\delta^{15}N$ signatures among scallop tissues: implications for ecology and physiology. J Exp Mar Biol Ecol 275:47–61

Lorrain A, Savoye N, Chauvaud L, Paulet YM, Naulet N (2003) Decarbonation and preservation method for the analysis of organic C and N contents and stable isotope ratios of low-carbonated suspended particulate material. Anal Chim Acta 491:125–133

Magen C, Chaillou G, Crowe SA, Mucci A and others (2010) Origin and fate of particulate organic matter in the southern Beaufort Sea–Amundsen Gulf region, Canadian Arctic. Estuar Coast Shelf Sci 86:31–41

Mayzaud P, Boutoute M, Noyon M, Narcy F, Gasparini S (2013) Lipid and fatty acids in naturally occurring particulate matter during spring and summer in a High Arctic fjord (Kongsfjorden, Svalbard). Mar Biol 160:383–398

McClintock JB (1994) Trophic biology of antarctic shallow-water echinoderms. Mar Ecol Prog Ser 111:191–202

McMeans BC, McCann KS, Humphries M, Rooney N, Fisk AT (2015) Food web structure in temporally-forced ecosystems. Trends Ecol Evol 30:662–672

McPhee MG, Proshutinsky A, Morison JH, Steele M, Alkire MB (2009) Rapid change in freshwater content of the Arctic Ocean. Geophys Res Lett 36:L10602

McTigue ND, Dunton KH (2014) Trophodynamics and organic matter assimilation pathways in the northeast Chukchi Sea, Alaska. Deep Sea Res II 102:84–96

McTigue ND, Bucolo P, Liu Z, Dunton KH (2015) Pelagic–benthic coupling, food webs, and organic matter degradation in the Chukchi Sea: insights from sedimentary pigments and stable carbon isotopes. Limnol Oceanogr 60:429–445

Meire L, Søgaard DH, Kortensen J, Meysman FJR and others (2015) Glacial meltwater and primary production are drivers of strong CO_2 uptake in fjord and coastal waters adjacent to the Greenland Ice Sheet. Biogeosciences 12: 2347–2363

Meire L, Meire P, Struyf E, Krawczyk DW and others (2016) High export of dissolved silica from the Greenland Ice Sheet. Geophys Res Lett 43:9173–9182

Meire L, Mortensen J, Meire P, Juul-Pedersen T and others (2017) Marine terminating glaciers sustain high productivity in Greenland fjords. Glob Change Biol 23: 5344–5357

Meziane T, Tsuchiya M (2000) Fatty acids as tracers of organic matter in the sediment and food web of a mangrove/intertidal flat ecosystem, Okinawa, Japan. Mar Ecol Prog Ser 200:49–57

Meziane T, Tsuchiya M (2002) Organic matter in a subtropical mangrove-estuary subjected to wastewater discharge: origin and utilisation by two macrozoobenthic species. J Sea Res 47:1–11

Middelbo AB, Sejr MK, Arendt KE, Møller EF (2018) Impact of glacial meltwater on spatiotemporal distribution of copepods and their grazing impact in Young Sound NE, Greenland. Limnol Oceanogr 63:322–336

Mincks SL, Smith CR, DeMaster DJ (2005) Persistence of labile organic matter and microbial biomass in Antarctic shelf sediments: evidence of a sediment 'food bank'. Mar Ecol Prog Ser 300:3–19

Mincks SL, Smith CR, Jeffreys RM, Sumida PYG (2008) Trophic structure on the West Antarctic Peninsula shelf: detritivory and benthic inertia revealed by $\delta^{13}C$ and $\delta^{15}N$ analysis. Deep Sea Res II 55:2502–2514

Moran SB, Lomas MW, Kelly RP, Gradinger R, Iken K, Mathis JT (2012) Seasonal succession of net primary productivity, particulate organic carbon export, and autotrophic community composition in the eastern Bering Sea. Deep Sea Res II 65-70:84–97

Murray C, Markager S, Stedmon CA, Juul-Pedersen T, Sejr MK, Bruhn A (2015) The influence of glacial melt water on bio-optical properties in two contrasting Greenlandic fjords. Estuar Coast Shelf Sci 163:72–83

Napolitano GE, Ackman RG (1992) Anatomical distributions and temporal variations of lipid classes in sea scallops *Placopecten Magellanicus* (Gmelin) from Georges Bank (Nova Scotia). Comp Biochem Physiol B 103:645–650

Napolitano GE, Pollero RJ, Gayoso AM, Macdonald BA, Thompson RJ (1997) Fatty acids as trophic markers of phytoplankton blooms in the Bahía Blanca estuary (Buenos Aires, Argentina) and in Trinity Bay (Newfoundland, Canada). Biochem Syst Ecol 25:739–755

Nérot C, Meziane T, Schaal G, Grall J, Lorrain A, Paulet YM, Kraffe E (2015) Spatial changes in fatty acids signatures of the great scallop *Pecten maximus* across the Bay of Biscay continental shelf. Cont Shelf Res 109:1–9

Ohashi Y, Iida T, Sugiyama S, Aoki S (2016) Spatial and temporal variations in high turbidity surface water off the Thule region, northwestern Greenland. Polar Sci 10: 270–277

Oxtoby LE, Mathis JT, Juranek LW, Wooller MJ (2016) Estimating stable carbon isotope values of microphytobenthos in the Arctic for application to food web studies. Polar Biol 39:473–483

Parrish CC (2009) Essential fatty acids in aquatic food webs. In: Arts MT, Brett MT, Kainz MJ (eds) Lipids in aquatic ecosystems. Springer, Dordrecht, p 309–326

Parrish CC, Thompson RJ, Deibel D (2005) Lipid classes and fatty acids in plankton and settling matter during the spring bloom in a cold ocean coastal environment. Mar Ecol Prog Ser 286:57–68

Pazos AJ, Sánchez JL, Román G, Luz Pérez-Parallé M, Abad M (2003) Seasonal changes in lipid classes and fatty acid composition in the digestive gland of *Pecten maximus.* Comp Biochem Physiol B 134:367–380

Pernet F, Tremblay R, Comeau L, Guderley H (2007) Temperature adaptation in two bivalve species from different thermal habitat: energetic and remodeling of membrane lipids. J Exp Biol 210:2999–3014

Peterson BJ, Fry B (1987) Stable isotopes in ecosystem studies. Annu Rev Ecol Syst 18:293–320

Piquet AMT, Van de Poll WH, Visser RJW, Wiencke C, Bolhuis H, Buma AGJ (2014) Springtime phytoplankton dynamics in Arctic Krossfjorden and Kongsfjorden (Spitsbergen) as a function of glacier proximity. Biogeosciences 11:2263–2279

R Core Team (2017) R: a language and environment for statistical computing. R Foundation for Statistical Computing, Vienna

Renaud PE, Tessmann M, Evenset A, Christensen GN (2011) Benthic food-web structure of an Arctic fjord (Kongsfjorden, Svalbard). Mar Biol Res 7:13–26

Reuss N, Poulsen LK (2002) Evaluation of fatty acids as biomarkers for a natural plankton community. A field study of a spring bloom and a post-bloom period off West Greenland. Mar Biol 141:423–434

Rhead MM, Eglinton G, Draffan GH, England PJ (1971)

Conversion of oleic acid to saturated fatty acids in Severn Estuary sediments. Nature 232:327–330

Ribeiro S, Sejr MK, Limoges A, Heikkilä M and others (2017) Sea ice and primary production proxies in surface sediments from a High Arctic Greenland fjord: spatial distribution and implications for palaeoenvironmental studies. Ambio 46(Suppl 1):106–118

Rysgaard S, Sejr MK (2007) Vertical flux of particulate organic matter in a High Arctic fjord: relative importance of terrestrial and marine sources. Medd Gronl Biosci 58: 110–119

Rysgaard S, Nielsen TG, Hansen BW (1999) Seasonal variation in nutrients, pelagic primary production and grazing in a high-Arctic coastal marine ecosystem, Young Sound, Northeast Greenland. Mar Ecol Prog Ser 179: 13–25

Rysgaard S, Vang T, Stjernholm M, Rasmussen B, Windelin A, Kiilsholm S (2003) Physical conditions, carbon transport, and climate change impacts in a northeast Greenland fjord. Arct Antarct Alp Res 35:301–312

Sampei M, Sasaki H, Forest A, Fortier L (2012) A substantial export flux of particulate organic carbon linked to sinking dead copepods during winter 2007–2008 in the Amundsen Gulf (southeastern Beaufort Sea, Arctic Ocean). Limnol Oceanogr 57:90–96

Savoye N, Aminot A, Tréguer P, Fontugne M, Naulet N, Kérouel R (2003) Dynamics of particulate organic matter δ^{15}N and δ^{13}C during spring phytoplankton blooms in a macrotidal ecosystem (Bay of Seine, France). Mar Ecol Prog Ser 255:27–41

Schomburg G (1987) Gaschromatographie Grundlagen, Praxis und Kapillartechnik, 2nd edn. Wiley-VCH, Weinheim, p 62–72

Schulz HD, Zabel M (2006) Marine geochemistry. Springer-Verlag, Berlin Heidelberg

Sejr MK, Jensen KT, Rysgaard S (2000) Macrozoobenthic structure in a high-Arctic East Greenland fjord. Polar Biol 23:792–801

Sejr MK, Stedmon CA, Bendtsen J, Abermann J, Juul-Pedersen T, Mortensen J, Rysgaard S (2017) Evidence of local and regional freshening of Northeast Greenland coastal waters. Sci Rep 7:13183

Silberberger MJ, Renaud PE, Kröncke I, Reiss H (2018) Food-web structure in four locations along the European shelf indicates spatial differences in ecosystem functioning. Front Mar Sci 5:119

Søreide JE, Tamelander T, Hop H, Hobson KA, Johansen I (2006) Sample preparation effects on stable C and N isotope values: a comparison of methods in Arctic marine food web studies. Mar Ecol Prog Ser 328:17–28

Søreide JE, Leu E, Berge J, Graeve M, Falk-Petersen S (2010) Timing of blooms, algal food quality and *Calanus glacialis* reproduction and growth in a changing Arctic. Glob Change Biol 16:3154–3163

Soudant P, Marty Y, Moal J, Robert R, Quéré C, Le Coz JR, Samain JF (1996) Effect of food fatty acid and sterol quality on *Pecten maximus* gonad composition and reproduction process. Aquaculture 143:361–378

Stead RA, Richoux NB, Pereda SV, Thompson RJ (2013) Influence of an intermittent food supply on energy storage by the subpolar deposit feeder *Yoldia hyperborea* (Bivalvia: Nuculanidae). Polar Biol 36:1333–1345

Tamelander T, Kivimäe C, Bellerby RG, Renaud PE, Kristiansen S (2009) Base-line variations in stable isotope values in an Arctic marine ecosystem: effects of carbon and nitrogen uptake by phytoplankton. Hydrobiologia 630:63–73

Thyrring J, Tremblay R, Sejr MK (2017) Importance of ice algae and pelagic phytoplankton as food sources revealed by fatty acid trophic markers in a keystone species (*Mytilus trossulus*) from the High Arctic. Mar Ecol Prog Ser 572:155–164

Vizzini S, Mazzola A (2003) Seasonal variations in the stable carbon and nitrogen isotope ratios (^{13}C/^{12}C and ^{15}N/^{14}N) of primary producers and consumers in a western Mediterranean coastal lagoon. Mar Biol 142:1009–1018

Wassmann P (2011) Arctic marine ecosystems in an era of rapid climate change. Prog Oceanogr 90:1–17

Editorial responsibility: James McClintock,
Birmingham, Alabama, USA

Submitted: July 24, 2018 ; Accepted: January 2, 2019
Proofs received from author(s): January 29, 2019